Optical spectrum based measurement of flotation slurry contents

Olli Haavisto *, Jani Kaartinen, Heikki Hyötyniemi

Helsinki University of Technology (TKK), Department of Automation and Systems Technology, P.O.Box 5500, FI-02015 TKK, Finland

ARTICLE INFO

ABSTRACT

Monitoring and control of a flotation circuit is mainly based on the information gained by assaying the process slurry lines. In flotation plants, usually an X-ray fluorescence analyzer is used to obtain the on-line assays. This article introduces the visual and near-infrared reflectance spectroscopic analysis of the process slurries as a supplementary method which complements the on-line assay information available from an X-ray fluorescence analyzer. It is shown that the spectral information can be used to accurately predict the element contents in the slurry in between successive XRF analyses. Since the spectral measurements can be taken with high frequency as opposed to the sparse X-ray fluorescence analysis, a practically continuous on-line estimate of the slurry contents is reached. These estimates can be used in the plant control to improve the overall performance of the circuits and to yield also economical savings. Additionally, the frequent monitoring of the grades can provide means to eliminate rapid disturbances in the circuits, thus improving the stability of the process.

1. Introduction

Mineral flotation is the most typical method for ore enrichment in the mining industry. The performance of flotation processes is monitored by measuring the element contents in the feed, concentrate and tailing slurry flows of the flotation cells. These measurements are also utilized in plant control. Additionally, the visual properties of the flotation froths in the cells are often monitored either directly by the operators or by using some automatic machine vision system. Especially color is generally agreed to roughly indicate the mineral content of the froth.

X-ray fluorescence (XRF) is commonly used for on-line measuring of elemental composition in industrial mineral flotation processes. In an XRF analyzer the slurry sample is radiated using X-rays, and the intensity of the fluorescence radiation of various elements in the sample is measured. Based on the fluorescence intensities at specific wavelengths the assay can be calculated. The XRF method provides accurate measures of the element contents but requires a quite extensive measurement equipment. Typically at flotation plants, one centralized analyzer is used to measure several slurry flow lines in turn. Assuming that there are over fifteen lines to be measured, the sampling interval of a single line increases to over 10 min. Usually this kind of cycle time is short enough to keep track of any disturbances due to the changes in the ore since the residence time in the flotation cells acts as a low pass filter. However, in a complex flotation circuit there may be other disturbance sources that are significantly faster. To compensate for this kind of changes with feedback control, a more

frequent concentration analysis is required. Otherwise the circuit may not be operated optimally.

Optical color measurements have been studied in the context of mineral composition analysis as a simple supplement or alternative for the XRF analyzers. Many studies have also concentrated on the visual analysis and classification of the flotation froths by machine vision, and color has often been one of the measured features (Bartolacci et al., 1998; Bonifazi et al., 2002; Hargrave and Hall, 1997; Kaartinen et al., 2006; Liu et al., 2005). Surprisingly, the color of flotation slurries has not been so intensively investigated. Oestreich et al. (1995) measured the color of artificial dry mineral mixtures, slurries of mineral mixtures and flotation froths using a video camera and correlated them with the mineral contents of the samples. It was detected that strong correlations exist between the color and the mineral contents. However, no experiments with real process samples were conducted.

Partly because of the interest in froth texture and also partly because of the lack of suitable optical spectral analyzers, the previously mentioned studies have mainly been using regular RGB cameras that provide only rough information on color. Recently, optical spectrometers capable of more accurate color measurements have been developed and utilized to mineral mixture analysis. Haavisto et al. (2006) measured the spectra of flotation froths in a real process environment and compared the results to color information gained from an RGB camera. The study concluded that the more accurate froth color information leads to better estimates of the froth element grades. Also slurry samples were analyzed and the results suggested that there exist correlations between the slurry spectra and the element contents. Additionally, a mineral analyzer produced by Blue Cube Systems based on the spectral analysis has been used in

* Corresponding author: Tel.: +358 9 451 6090; fax: +358 9 451 5208.
  E-mail address: olli.haavisto@tkk.fi (O. Haavisto).

heavy mineral sands separation plants for the analysis of dry mineral mixtures (De Waal and Du Plessis, 2005).

In general, the concept of measuring the optical spectrum of light reflected from a sample is referred as *optical reflectance spectroscopy* (Clark, 1999). The specific form of the reflected light spectrum, i.e. the color of the material is a result of the absorption properties of the molecular structure of that specific material.

This study concentrates on the visible and near-infrared (VNIR) reflectance spectroscopic analysis of slurry in mineral flotation. Earlier operator interviews (Hätönen, 1999) have indicated that especially in zinc flotation the visual inspection of froth color can be used to roughly estimate the zinc grades. Thus, the zinc circuit was selected as the starting point for the analysis. First, some laboratory tests are introduced showing the effect of changing slurry element contents in the different zinc slurry spectra. Then, a prototype of an on-line measurement device is presented that is used to measure the spectrum of the flowing slurry in a real flotation plant environment. Statistical multivariate methods are applied to the measured data to create a model between the spectral measurements and the element contents of the slurries provided by the XRF analyzer. It is shown that the spectra obtained by the simple and fast spectral measurement system actually contain very specific information on the composition of the slurry. Thus the sparse assays provided by the XRF analyzer can be complemented with the frequent estimates calculated using the spectra to obtain a comprehensive prediction of the current contents of the slurry line. The frequent content estimates provide useful monitoring information on fast changes of the circuits.

2. Methods

2.1. Application environment

The on-line measurements for this study were conducted at the concentrator plant of Inmet Mining Corporation's Pyhäsalmi copper, zinc and pyrite mine, located in Pyhäjärvi town, central Finland. The concentration process of the mine starts with screening and grinding of the hoisted ore. After grinding, the process comprises three concatenated flotation circuits, one for each main mineral. The main slurry lines and some intermediate products in the circuits are measured each in turn by a single XRF analyzer (Outotec Courier® 6 SL), resulting to a sampling interval of about 18 min for altogether 24 sample lines. These measurements are used by the operators and the automatic control system of the plant to monitor the process and to regulate the amount of added flotation reagents, flotation cell aeration rates and pulp levels.

The XRF analyzer at Pyhäsalmi concentrator is a centralized one, meaning that a separate primary sampling line is sampled and transported from each measured slurry line to the analyzer for the assaying. From the final zinc concentrate, the iron, copper and zinc contents are measured. Additionally, the sulphur content is estimated as a linear combination of the iron and zinc contents based on the knowledge of the compositions of the main minerals present in the ore.

2.2. Spectral measurement equipment

Spectral measurements were carried out using an imaging spectrograph (Specim ImSpector V10) mounted to a monochrome CCD camera (Basler A102f). The spectral images are formed by passing light from imaging optics to the spectrograph through an entrance slit. The obtained line is transformed into a 2D image by passing the light through a prism-grating-prism (PGP) component. The spectrograph used in this study operates in VNIR with wavelength range of 400–1000 nm and is equipped with an order blocking filter (OBF), which is used to filter out unwanted higher order spectra.

Main criteria for the camera selection was a good enough spectral response and spatial resolution as well as an affordable price. The spectral response shown in Fig. 1 is good enough for the purposes of this study, although the higher wavelengths suffer from diminished sensitivity. The spatial resolution of the camera is 1280×960 pixels, which is more than enough in vertical direction since the spectral resolution of the spectrograph is 9 nm. The horizontal dimension is related to position along the line and is not important in this case because only one spectrum is currently used for the analysis. Thus, the spectra along the whole line are averaged to form the final spectral measurement.

An imaging spectrograph was used because in the future it can be easily extended to measure many slurry samples by replacing the regular optics with optical fibers. This way the same measurement equipment will be applicable to the case where several slurry lines are measured simultaneously.

2.3. Laboratory tests

At the beginning there was a need to get assurance of the power of the proposed method before on-line factory scale analysis. Thus, the
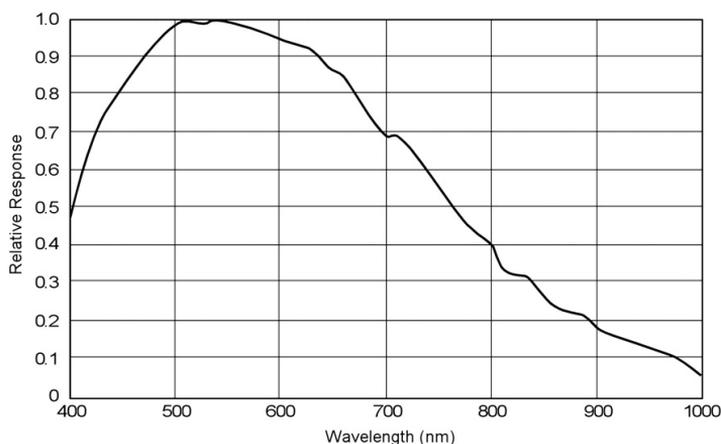

Fig. 1. Relative spectral response of the CCD camera with respect to the wavelength (Figure courtesy of Basler Vision Technologies).

very first tests were conducted in laboratory with test samples collected from the plant. The samples were approximately 5 l in volume and they were circulated continuously in a system consisting of a small tank, an adjustable pump and a jet flow cell similar to one used in commercial Courier® XRF analyzers (see Fig. 2). The jet flow cell is designed to cause appropriate turbulence to the incoming flow which results to a representative sample over the window area. Spectral analysis was conducted by illuminating the flow cell window with a lamp and measuring the light reflected from the sample with the spectrophotometer. After testing different measurement setups (illumination, imaging conditions and flow cell windows) it was concluded that only the obvious factors had a significant impact on the spectrum: the spectrum of the illuminating lamp should be wide enough and the illumination geometry should be selected in a way that total reflection from the window is minimized. In the selected setup illumination is done with a single halogen lamp (12 V, 50 W, 4700 K) and a clear 50 μm mylar film is used as a flow cell window.

The analysis was done by preparing a batch of a sample for circulation, measuring the spectra and washing the system thoroughly with water before the next sample. All the samples described here were also analyzed with different solids content (SC) values in order to find out if that would have a significant influence on the spectra. The solids content was altered by starting the analysis with the highest SC values and diluting the continuously flowing sample with water. The results obtained from the laboratory tests are presented in Section 3.1.

2.4. On-line spectral measurement setup

Since the first pilot test was a success a prototype capable of performing on-line measurements was built. It is connected to a primary sampling line of the on-line XRF analyzer as shown in Fig. 3. The spectral analysis equipment and positioning is similar to the one described above. The only modification was that the thin film window that must be used in the XRF analyzer to pass X-ray radiation through
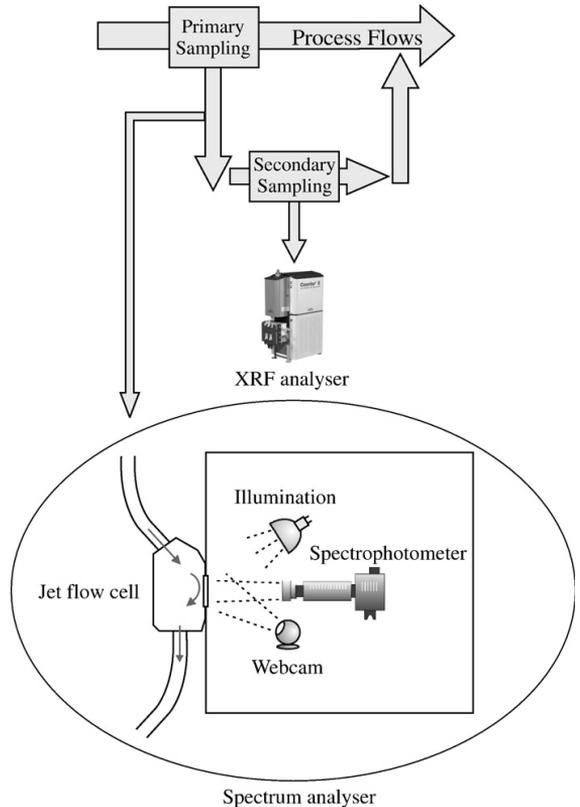

Fig. 2. Pilot test equipment.
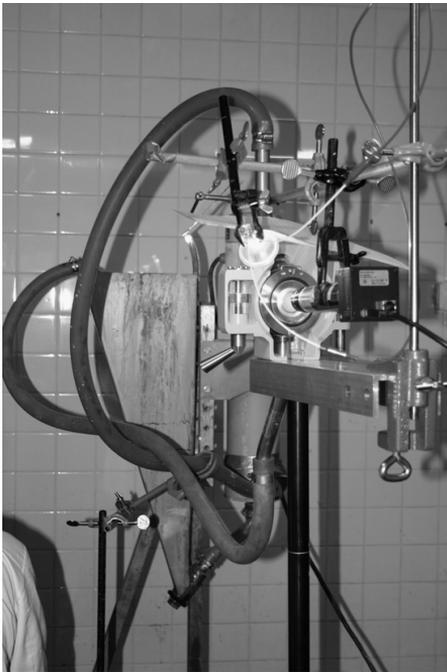

Fig. 3. Sampling point and a schematic diagram of the on-line analyzer.

could be replaced with a durable sapphire window. This made the on-line setup practically maintenance free once the slurry flow was running through the flow cell.

The camera is connected to a desktop PC that has a local area connection to the ethernet network and automation system of the plant. All the equipment are placed in a protective housing (Fig. 4) that is kept in a slight overpressure in order to keep the instruments clean. The incoming air is filtered and additional dried instrument air flow is directed to the jet flow cell window to prevent condensing.

Furthermore, there are remote operating capabilities via the Internet as well as an additional web camera monitoring the jet flow cell window. This makes it possible to check the status of the system and make algorithm updates remotely. To reduce the risk of damages in case of a leakage, the flow cell is placed outside of the protective housing and only the window is visible from inside.

2.5. On-line data preprocessing

On-line optical spectral data were gathered from the zinc concentrate line for an eight day period using a sampling interval of 10 s. During this time the process was normally operated and typical grade changes occurred. For improved data collection, the XRF analyzer was configured to measure the zinc concentrate assay with double the frequency, so that the sampling interval of the line was approximately 9 min. The doubled XRF sampling frequency allowed every other sample to be reserved for validation purposes, as explained in Section 3. As a result, a set containing 66 420 spectra and 1100 grade measurements was obtained.
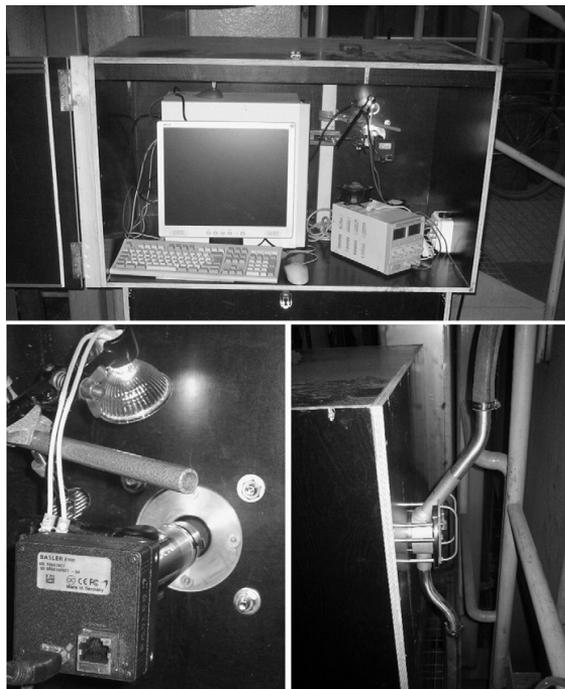
Fig. 4. Prototype of the on-line analyzer.

The original dimension of one spectral measurement obtained from the spectrophotometer equalled the vertical resolution of the camera (960 pixels). However, since the spectral resolution of the spectrophotometer was as large as 9 nm, the intensity vector dimension was reduced to 20 by averaging each 48 neighboring intensity values. This operation did not affect the modeling performance but it reduced the required computational load.

The secondary sampling unit in the XRF analyzer collects the actual slurry sample from the continuous primary sample flow during a 30 s long period. Thus it can be assumed that the assays represent the average of the element contents in the primary sample flow during this period. To mimic the averaging in the spectrum measurements, for each spectrum the average of the current and two previous spectra was calculated, and the original measurements were replaced by these values in the further analysis. To form the necessary XRF and spectrum sample pairs for model calculation, a constant delay between the spectral and XRF measurement was assumed, so that for each sparse XRF sample a corresponding spectrum could be picked from the spectrum data set.

The color intensities seen on the flow cell window of the spectral measurement system are due to the reflections from separate mineral particles in the slurry. It is obvious that the dependence of the measured light intensity of the elemental concentrations in the solids is nonlinear in nature; light is reflected only by the mineral surfaces that are visible to the light source and the spectrograph immediately at the surface behind the window. With the laboratory results it turned out that most of the nonlinearity was compensated by a straightforward exponential transformation. The measured intensities were raised to the power of 3/2. This kind of linearization step was used throughout the analysis.

The predictor and response data were scaled by dividing each variable with its standard deviation. Instead of removing the mean values, an additional constant predictor variable was added to each

spectrum vector. This was convenient later in the recursive estimation case since the estimation and removal of the mean values was thus coded inside the model.

2.6. Partial least squares regression

The standard multivariate regression (MLR) based on the least squares fitting is not suitable for data sets where the predictor variables have strong correlations with each other (Hyötyniemi, 2001), like in this case of the smooth spectrum values. The situation can be remedied by mapping the predictors (collected in vector $x(k)$) first into a lower dimensional latent variable space, from which the final mapping to the response space is performed. This principle is used e.g. in principal component regression (PCR) and partial least squares regression (PLS). In this study, the PLS approach was selected because it considers both predictor and response data when determining the optimal latent space used in the mapping. Since the required mappings are linear, the final PLS model can be described as one matrix B which connects the predictors to the responses:

$$y(k) = Bx(k) + f(k), \qquad (1)$$

where $x(k)$ refers to the predictor column vector (spectrum) and $y(k)$ to the response column vector (element and solids contents) of the k:th data sample. The column vector $f(k)$ contains the modeling error. For more information on the PLS regression, the reader is referred to Wold et al. (2001).

Typical industrial processes are non-stationary or time-varying. Thus a static PLS model calculated from a fixed data set is not valid for longer term usage. To overcome this restriction, a recursive PLS (rPLS) algorithm was introduced by Helland et al. (1991) and improved by Qin (1993), Dayal and MacGregor (1997), and Qin (1998). The idea of rPLS is to recursively update the original PLS model using new data points. Usually also some forgetting scheme is included, so that the newer data points are affecting more in the current mapping whereas the older ones are gradually forgotten.

For this study, the fast kernel-based rPLS algorithm presented by Dayal and MacGregor (1997) was applied to the measured data. The recursive part of the algorithm is realized by updating the (unscaled) predictor covariance matrix, R_{xx}, and the (unscaled) crosscovariance matrix of the predictors and responses, R_{xy}, as follows:

$$R_{xx}(k) = \lambda R_{xx}(k-1) + x(k)x^T(k), \qquad (2)$$

$$R_{xy}(k) = \lambda R_{xy}(k-1) + x(k)y^T(k), \qquad (3)$$

where $(\cdot)^T$ denotes the transpose. This corresponds to exponential weighting of the samples with the forgetting factor λ. To describe the effect of forgetting, the memory time constant $T_0(\lambda)$ of the decreasing of the weights can be calculated (Ljung, 1999):

$$T_0(\lambda) = \frac{1}{1-\lambda}, \qquad (4)$$

meaning that it is assumed that the system remains constant for approximately $T_0(\lambda)$ samples.

3. Results

The results of this study can be divided into three main categories. At first, the results from the laboratory tests are presented and analyzed. Then, the on-line data containing the spectra and the XRF values are modeled using an ordinary, non-recursive PLS model. The quality of the model is judged by the root mean square of the estimation error for the validation data set. Using this non-recursive PLS model, the time delay between the spectral and XRF measurements is estimated to synchronize the measurements as well

Table 1
Laboratory analysis for the collected zinc circuit samples

	Zn%	Cu%	S%	Fe%	Pb%
Rougher	45.39	0.29	31.3	12.0	0.20
Scavenger	12.43	0.71	29.7	26.0	0.22
Cleaner	56.44	0.32	32.5	8.5	0.22

as possible. After that, the optimal number of latent variables for the PLS mapping is determined.

The third part of the results deals with the recursive PLS modeling as a method for continuous on-line grade value estimation. The recursive approach has to be utilized because it turns out that the system is not stationary.

3.1. Laboratory tests

The samples for the preliminary laboratory tests were collected from the froth lip of the zinc rougher, scavenger and cleaner flotation cells of the Pyhäsalmi concentrator during a normal operation of the plant. They were split into two parts, one for the plant laboratory and the other for spectral analysis conducted in the Outotec's test laboratory. The results of the laboratory analysis are shown in Table 1. As can be seen, there are large variations in the element contents, especially for zinc and iron, which were expected to be seen in the spectra.

Fig. 5 shows the results for the analysis of the zinc circuit samples. There are eleven spectra in total that are drawn with three different line types depending on the origin of the sample. The used solids content values for each sample are shown in the legend texts. As can be seen, the changes in the mineral content are dominating the shape of the spectrum, whereas the variation in the solids content has a minor effect (emphasized on the small sub-figure). This explains why the reflectance spectroscopy is not so reliable in predicting the solids contents as they are with the elements — as described later in Section 3.3.
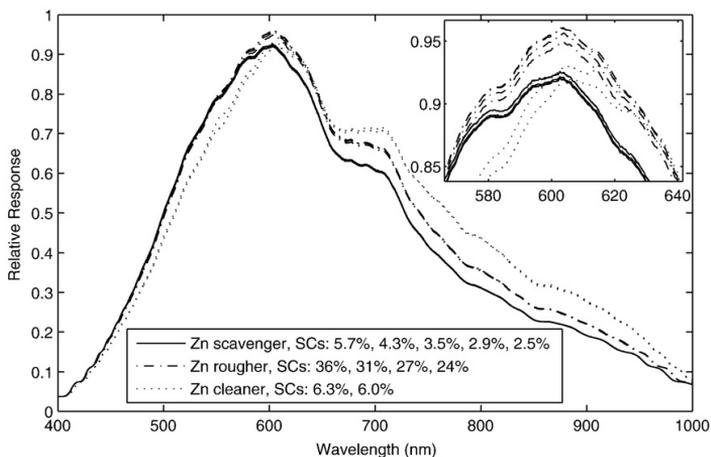
3.2. Delay and model order

After the promising laboratory results, the study was continued with the on-line data collected from the final zinc concentrate. The
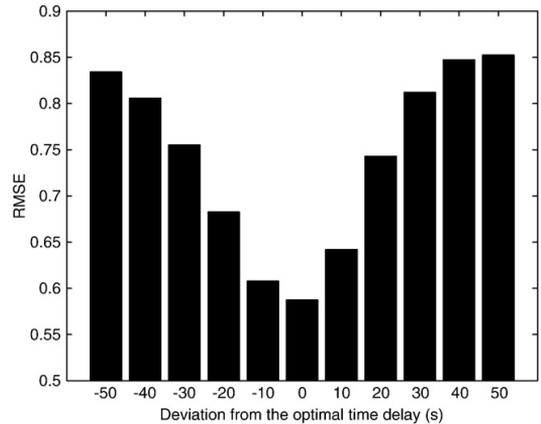
Fig. 6. Temporal synchronization of the spectral and XRF measurements affects strongly the root mean square error for the validation data.

complete data set was divided into three parts: Every other sample of the first half of the data was used for estimation, and the samples in between formed the validation data. The second half of the data was entirely reserved for testing, and is referred in the following as the test data set.

Based on the measurement setup, the time delay between the time stamps given by the XRF analyzer and the spectral measurement system for the same slurry sample could not be determined. The delay had to be estimated from the data. Non-recursive PLS models were calculated using the estimation data set and the corresponding spectral measurements with different constant delays between the spectra and the XRF measurements. Fig. 6 shows the averaged root mean squared error (RMSE) between the measured and estimated grades of all the element species and the solids content for the validation data, when the time delay used in the modeling was varied around the optimal value. Clearly it is very important to synchronize the measurements correctly, since already a deviation of 20 s increases the estimation error considerably. This also suggests that the content values are varying quite rapidly and that measurements with a high

Fig. 5. Spectral responses for different flotation cells and solids contents (SC). The peak area is emphasized in the top right hand corner.
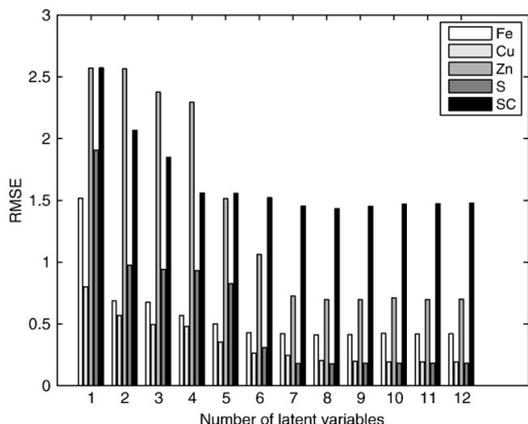
Fig. 7. Modeling error of validation data with respect to the number of latent variables in the PLS model.

Table 2
Root mean square errors (RMSE) in percentage points for the non-recursive PLS model (validation and test data sets) and for the recursive PLS (rPLS) model compared with the data mean and standard deviation

	PLS RMSE (validation)	PLS RMSE (test)	rPLS RMSE	Data mean	Data std
Fe	0.41	1.00	0.33	9.91	1.27
Cu	0.24	1.02	0.16	0.87	0.78
Zn	0.68	1.64	0.56	52.39	2.17
S	0.18	0.45	0.14	34.16	0.52
SC	1.52	4.10	1.39	36.43	2.42

3.3. Model analysis

Once the model structure was determined, the modeling performance was analyzed by comparing the measured and estimated content values for the validation data. Fig. 8 shows a typical sample of these results. Only the validation samples are shown, and the estimation samples between them are omitted. Clearly the overall performance of the model is very good; the actual modeling errors for the whole validation data set are shown in the first column of Table 2. Based on these results it is already possible to conclude that the spectral measurements provide a promising supplement for assaying mineral slurries. Also the solids content can be predicted from the spectra, even though with quite poor accuracy.

In order to determine the importance of different wavelengths for the estimation, the model coefficients in matrix B can be analyzed (Fig. 9). Evidently the whole spectral range is used by the model and can thus be assumed to carry information on the response variables. However it seems that the importance of different wavelengths is varying quite heavily. The coefficients related to iron and zinc have a strong resemblance, only with an opposite sign. This is natural because the relative content values are used; if the zinc grade increases there is more sphalerite in the slurry, which decreases the iron grade since less pyrite and chalcopyrite is present. Also the

sampling frequency are required to follow these changes. The model of order nine was used in the delay estimation to ensure that all the important properties of the data were captured by the model.

In addition to the optimal time delay, also the optimal number of latent variables (i.e. the PLS model order, see Section 2.6) was determined using the non-recursive PLS model. Fig. 7 shows the RMSE of the validation data for different model orders with the optimal delay. The best possible modeling performance is almost reached already with seven latent variables. However, by using eight variables slightly better results are obtained. Thus, in the following analysis the model order eight was utilized.
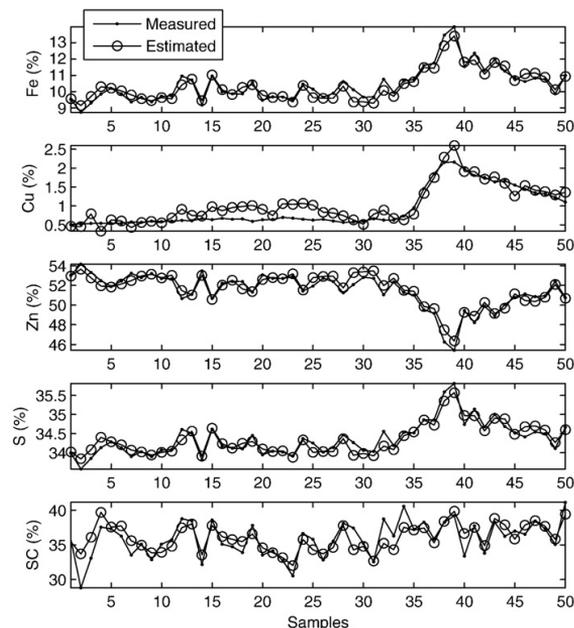

Fig. 8. Measured and estimated contents for a typical sample of the validation data. The time period of the shown data series is about 15 h.
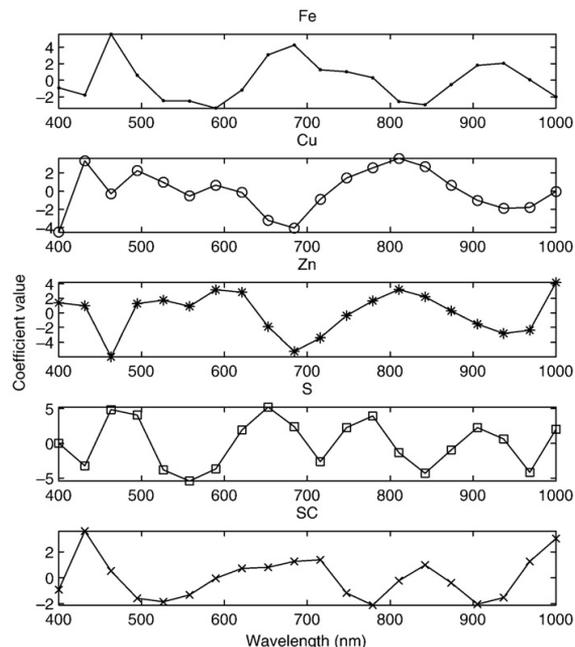

Fig. 9. Constant PLS model coefficients with respect to wavelength.

copper and zinc coefficients are close to each other, the main differences being on the wavelength range 400–500 nm. On the both extremes (near 400 and 1000 nm) the absolute values of the spectrum are small (see Fig. 5). This may cause numerical problems which further affect the corresponding model coefficient values, thus explaining the sharp changes of the coefficients near these wavelengths.

As mentioned in Section 3.2, the non-recursive PLS model was calculated and validated using the first half of the whole data set. This data covered a period of 3 days and 10 h. The same model was then applied to the test data set (second half of the whole data) to test the model generalization ability. The results (Fig. 10, second column of Table 2) clearly show that the constant model quite quickly loses the ability to predict the grades when applied to new data. About five or six of the first test samples are estimated well, but after that the prediction gradually becomes biased. Consequently, as the sampling interval in Fig. 10 is about 9 min, the model remains valid for about an hour.

The gradual changes in the relation between the color and the grades are due to the changing properties of measured slurry that are not related to the elemental composition. Evidently some of the variation is due to varying mineralogy in the mine. Also the upstream processes can cause changes. At least the following properties typically vary:

(1) exact chemical compositions of the minerals
(2) particle size distribution
(3) grain size distribution
(4) amount of locked particles

The XRF analysis is based on atomic phenomena and measures the element composition of the slurry sample and is not so sensitive to these factors. The optical reflectance spectrum, on the other hand, is determined by the light absorption properties of the mineral particles in the sample. Since the minerals consist of varying non-stoichio-
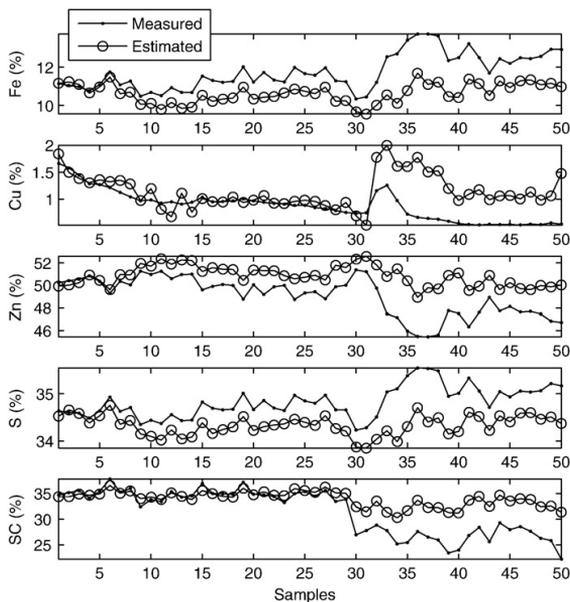
metric compounds (for example, in Pyhäsalmi sphalerite (ZnS) typically contains also 7–8% of iron) it is possible that two samples with very similar element compositions have different spectra. Also the particle and grain size distributions have their effect on the colour of the reflected light: if the grains or particles are small, an average photon has to scatter many times before it is (possibly) reflected back to the spectrometer. This increases the probability of absorption and amplifies the influence of dark minerals on the spectrum (Clark, 1999).

However, as shown by the previous results, the changes in the incoming ore appeared to be relatively smooth so that it was possible to calculate a model that momentarily connects the spectral information and the element contents of the slurry. To further exploit this observation, a recursive modeling approach was applied to the data.
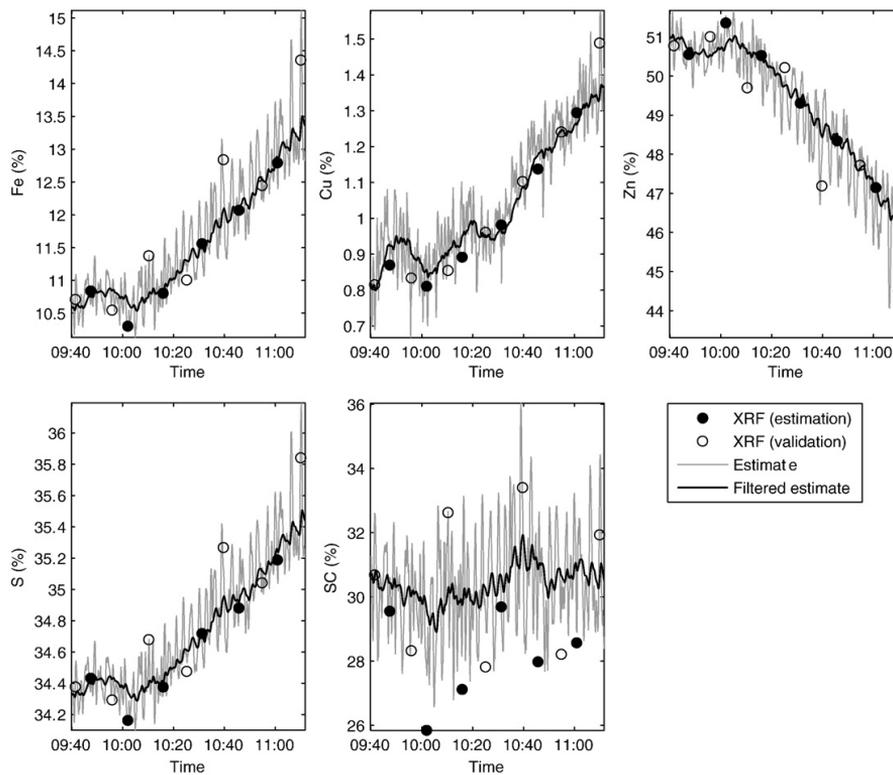
3.4. Recursive PLS model

In the recursive approach the PLS model is updated on-line after each new XRF analysis and spectrum sample pair is obtained. This way the model should always describe the current relation between the spectrum and the corresponding contents of the slurry, assuming that the changes in the system are smooth enough. The recursive PLS algorithm (see Section 2.6) was applied to the same data set as previously using eight latent variables and a forgetting factor value $\lambda = 0.96$, which according to Eq. (4) corresponds to a memory time constant $T_0(0.96) = 25$ samples. One hundred matching XRF and spectrum sample pairs from the beginning of the data set were used purely for estimation to initialize the recursive PLS model. After that, again only every second sample pair was used to update the recursive model, whereas the other sample pairs were reserved for validation. Because of the doubled XRF sampling frequency, this enabled the measuring of the prediction performance of the recursive model between two ordinary XRF measurements. However, as opposed to the validation of the non-recursive PLS model, this time the model was calculated on-line using only the previously obtained XRF and spectrum sample pairs.

As shown in Table 2, the recursive PLS model provides the best alternative for estimating the assays from the spectra. Predictions for the validation samples are even better than the ones given in the validation of the non-recursive PLS model. These results indicate that it is possible to accurately estimate the slurry contents on-line from the spectral data by constantly updating the PLS model with the latest available XRF measurement.

Since it is easily possible to reach as short sampling interval as 10 s for the spectrum and a valid PLS model is always provided by the recursive algorithm, a practically continuous assay of the slurry line is obtained as demonstrated in Fig. 11. The data shown in the figure represents a situation where the zinc content of the final zinc concentrate starts to fall, whereas the copper content increases indicating a disturbance in the flotation process. Clearly the predicted content values agree well with both the estimation and validation XRF samples, as already shown.

One important observation directly seen from Fig. 11 is that there are rapid oscillations present in each content value. This explains the importance of the temporal synchronization of the XRF and spectral measurements. However, it also reveals that the original XRF measurements which use a 30 s long slurry sample provide only a very instantaneous assay of the slurry. For the plant monitoring and control, more important would be to know the general behaviour of the element content variations. Now, because of the high sampling frequency of the spectrum it is easy to calculate a low-pass filtered estimate representing the averaged contents of the slurry at the current time. This was done by exponentially filtering the original estimate. Naturally, since the filtered estimate is an average over many measurements, it provides a much more reliable assay than the instantaneous and sparse values provided by the XRF analyzer alone

Fig. 10. Estimation results of the constant PLS model for the first 7.5 h of the test data set. The model was calibrated with the estimation data collected immediately before the shown test data. The sampling interval of the data is about 9 min.

Fig. 11. Original sparse XRF measurements can be completed with the frequent estimates calculated from the spectra. The normal sampling interval of the XRF analyzer is about 18 min. However, during this experiment, doubled sampling frequency was used to collect also the validation samples. The sampling interval of the spectrum and the estimate was 10 s, and 90% exponential filtering was used to calculate the filtered estimate.

(Fig. 11). As a consequence, the more accurate and frequent assays should also improve the performance of the circuit if utilized in control instead of the traditional XRF measurements.

Additionally, the frequent assaying of slurry lines provides new information on the dynamic behaviour of the flotation circuit. For example, the fast oscillations of the content values shown in Fig. 11 cannot be seen from the sparse XRF measurements alone. It is evident that these oscillations are caused somewhere earlier in the zinc circuit, and it seems that the alternating overflow of the roughing and middlings roughing cell banks is the primary reason for them together with the slow single input PID control loops for the cell levels. From the plant control point of view, detecting and eliminating this kind of oscillations would improve the overall performance of the circuit by stabilizing the flotation conditions in the cells.

In Pyhäsalmi mine, the spectral measurements of the zinc concentrate are currently provided for the process operators for monitoring purposes. However, in the future the improved assays will be utilized also in the plant control.

4. Conclusion

A relatively straightforward method for on-line measuring the VNIR spectrum of mineral flotation slurry was presented in this study. It was shown that the spectral information can be used to predict the temporary element and solids contents of the slurry in a zinc flotation circuit within a limited period of time. Because of the high sampling frequency of the spectrophotometer, a practically continuous estimate

for the contents of the final zinc concentrate slurry line was obtained. This estimate reveals the high-frequency oscillations that the XRF analyzer is unable to detect, thus providing means to improve the process performance by eliminating these disturbances. Furthermore, the low-pass filtered estimate serves as a reliable assay of the major content variations in the slurry.

The results showed that the relationship between the slurry spectrum and the element contents of the zinc concentrate in Pyhäsalmi mine does not remain constant for longer periods of time because of the changes in the slurry properties. That is why regular reference measurements from the XRF analyzer were required to update the recursive PLS model which maps the spectrum to the assay. However, it seems that the necessary changes in the model are relatively smooth, so that the newest model is valid longer than the typical sampling interval of the XRF analyzer. A reference is required within 1 h to keep the assay from drifting from the XRF analyses.

In a more general level, this study confirms that the VNIR range spectrum of the flotation slurry definitely is a beneficial indicator of the element contents at least in the case of zinc flotation. When applied together with the XRF analyzer, the spectral measurements can notably improve the assaying of flotation slurries.

References

Bartolacci, G., Pelletier Jr., P., Tessier Jr., J., Duchesne, C., Bossé, P.-A., Fournier, J., 1998. A real time visual sensor for supervision of flotation cells. Miner. Eng. 11 (6), 489–499.

Bonifazi, G., Massacci, P., Meloni, A., 2002. A 3D froth surface rendering and analysis technique to characterize flotation processes. Int. J. Miner. Process. 64 (2–3), 153–161.

Clark, R.N., 1999. Spectroscopy of rocks and minerals, and principles of spectroscopy. In: Rencz, A.N. (Ed.), Manual of Remote Sensing, vol. 3. John Wiley and Sons, New York, pp. 3–58. Ch. 1.

Dayal, B., MacGregor, J., 1997. Recursive exponentially weighted PLS and its applications to adaptive control and prediction. J. Process Control 7 (3), 169–179.

De Waal, P., Du Plessis, F.E., 2005. Automatic control of a high tension roll separator. In: Akser, M., Elder, J. (Eds.), Heavy Minerals Conference Proceedings 2005. Society of Mining, Metallurgy, and Exploration, pp. 241–249.

Haavisto, O., Kaartinen, J., Hyötyniemi, H., 2006. Optical spectrum based estimation of grades in mineral flotation. Proceedings of the IEEE International Conference on Industrial Technology (ICIT 2006), Mumbai, India, pp. 2529–2534.

Hargrave, J., Hall, S., 1997. Diagnosis of concentrate grade and mass flowrate in tin flotation from colour and surface texture analysis. Miner. Eng. 10 (6), 613–621.

Hätönen, J., 1999. Image analysis in mineral flotation. Tech. Rep. 116, Helsinki University of Technology, Control Engineering Laboratory.

Helland, K., Berntsen, H., Borgen, O., Martens, H., 1991. Recursive algorithm for partial least squares regression. Chemom. Intell. Lab. Syst. 14, 129–137.

Hyötyniemi, H., 2001. Multivariate regression — techniques and tools. Tech. Rep. 125, Helsinki University of Technology, Control Engineering Laboratory.

Kaartinen, J., Hätönen, J., Hyötyniemi, H., Miettunen, J., 2006. Machine-vision-based control of zinc flotation — a case study. Contr. Eng. Pract. 486 (14), 1455–1466.

Liu, J., MacGregor, J., Duchesne, C., Bartolacci, G., 2005. Flotation froth monitoring using multiresolutional multivariate image analysis. Miner. Eng. 18 (1), 65–76.

Ljung, L., 1999. System Identification, Theory for the User, 2nd Ed. Prentice Hall PTR, Upper Saddle River, NJ.

Oestreich, J., Tolley, W., Rice, D., 1995. The development of a color sensor system to measure mineral compositions. Miner. Eng. 8 (1/2), 31–39.

Qin, S., 1993. Partial least squares regression for recursive system identification. Proceedings of the 32nd Conference on Decision and Control, San Antonio, Texas, pp. 2617–2622.

Qin, S., 1998. Recursive PLS algorithms for adaptive data modeling. Comput. Chem. Eng. 22 (4/5), 503–514.

Wold, S., Sjöström, M., Eriksson, L., 2001. PLS-regression: a basic tool of chemometrics. Chemom. Intell. Lab. Syst. 58, 109–130.